

Effects of the formation time of parton shower on jet quenching in heavy-ion collisions

Mengxue Zhang,^{1,2} Yang He,^{1,2} Shanshan Cao,^{1,2,*} and Li Yi^{1,2,†}

¹*Institute of Frontier and Interdisciplinary Science,
Shandong University, Qingdao, Shandong 266237, China*

²*Key Laboratory of Particle Physics and Particle Irradiation of Ministry of Education,
Shandong University, Qingdao, Shandong, 266237, China*

(Dated: August 30, 2022)

Jet quenching has successfully served as a hard probe to study the properties of the Quark-Gluon Plasma (QGP). As a multi-particle system, jets take time to develop from a highly virtual parton to a group of partons close to mass shells. In this work, we present a systematical study on the effects of this formation time on jet quenching in relativistic nuclear collisions. Jets from initial hard scatterings are simulated with Pythia and their interactions with the QGP are described using a Linear Boltzmann Transport (LBT) model that incorporates both elastic and inelastic scatterings between jet partons and the thermal medium. Three different estimations of the jet formation time are implemented and compared, including instantaneous formation, formation from single splitting and formation from sequential splittings, before which no jet-medium interaction is assumed. We found that deferring the jet-medium interaction with a longer formation time not only affects the overall magnitude of the nuclear modification factor of jets, but also its dependence on the jet transverse momentum.

I. INTRODUCTION

Quark-gluon plasma (QGP) is a state of matter in which quarks and gluons are deconfined instead of being bounded inside hadrons [1–3]. Relativistic heavy-ion collisions provide a unique laboratory to study the properties of QGP [3], and jet quenching is among the major signatures of the creation of QGP in these energetic collisions [4–6]. The observed suppression of the high transverse momentum (p_T) hadron and reconstructed jet spectra is considered a consequence of both elastic and inelastic scatterings between the energetic partons produced via initial hard collisions and the color-deconfined QGP medium [7–20]. The amount of energy transferred between jet partons and the QGP is governed by a set of transport coefficients, such as the strong coupling parameter α_s and the jet quenching parameter \hat{q} [21, 22]. And it is still an ongoing effort to extract these parameters from the jet quenching data, such as the nuclear modification factor [23–25], which helps quantify the transport properties or the opacity of the QGP medium.

With tremendous efforts on systematical experimental measurements and ever more sophisticated theoretical calculations, studies on jet-medium interactions have been extended from nuclear modification of high p_T hadrons [26–33] and jets [34–46], to the intra-structures of jets [47–59] as well as the jet-related correlations [60–69]. In most of these studies, jet production in heavy-ion collisions are usually factorized into three stages: parton production and shower in vacuum (or proton-proton collisions), interaction with the QGP and hadronization. However, different assumptions have been adopted for

the starting time of jet-medium interactions. This could introduce uncertainties in evaluating the nuclear modification on jets and has attracted several investigations in recent literature [70, 71]. For instance, this starting time has shown to affect the azimuthal dependence of jet quenching [71]. And with a time reclustering algorithm, jets with longer formation time exhibit a weaker quenching [70].

In this work, we will conduct a detailed study on the effects of the jet formation time on jet energy loss. The initial jets prior to interacting with the QGP are generated from Pythia 8 simulation [72, 73]. Due to the lack of the information on the jet formation time from Pythia, we designed three different evaluations on the production time of each parton within jets, varying from zero formation time, to an estimation based on a single splitting before formation, and a more elaborate estimation for a sequence of multiple splittings generated in Pythia. Interactions between these jet partons and the QGP are then simulated using a linear Boltzmann transport (LBT) model [32, 74] that describes both elastic and inelastic scatterings between jet partons and thermal partons from the QGP. Within this framework, we investigate how different estimations of the jet parton formation time affects the nuclear modification of fully reconstructed jets at the RHIC energy, and find that different modelings of this formation time impact not only the overall magnitude but also the p_T dependence of the nuclear modification factor of jets. The goal of the present study is to explore the sensitivity of jet quenching to the starting time of parton-medium interactions. For a more comprehensive discussion on the LBT model and its comparison to various experimental data, one may refer to Refs. [32, 33, 44, 45, 54, 59, 65, 68, 74, 75].

The remainder of this paper will be organized as follows. In Sec. II, we will discuss how the parton shower generated by Pythia is utilized to estimate the forma-

*Electronic address: shanshan.cao@sdu.edu.cn

†Electronic address: li.yi@sdu.edu.cn

tion time of each parton, and study the dependence of the formation time on the parton energy. In Sec. III, we will investigate effects of formation time on the nuclear modification factor (R_{AA}) and the central-to-peripheral ratio (R_{CP}) of jets in heavy-ion collisions using the LBT model. In the end, we will summarize in Sec. IV.

II. MODELINGS OF THE PARTON FORMATION TIME

We use the Pythia 8 event generator to simulate jet parton production and its vacuum shower. Since initial parton production processes – e.g. multi-parton interaction (MPI) – other than the hardest scattering are also shown essential in describing the jet observables, especially those related to soft particles [68, 76], we feed the full Pythia events of final-state partons into the LBT model for their subsequent interactions with the QGP. In hard scatterings, a pair of highly virtual partons are first created, which continue splitting until virtuality of each daughter is sufficiently low – close to its mass shell or approaching the scale of hadronization. We will use the mother-daughter tree provided by the Pythia shower to evaluate the time taken by each splitting, thus obtain the formation time of each parton in the end.

For a $1 \rightarrow 2$ process, the splitting time can be estimated using the uncertainty principle as [77]

$$\tau_{\text{form}} = \frac{2Ex(1-x)}{k_{\text{T}}^2}, \quad (1)$$

in which E represents the energy of the mother parton, x and $(1-x)$ are the energy fractions taken by the two daughters, and k_{T} is the transverse momentum of the daughters with respect to their mother. Here, the rest masses of both mother and daughters are neglected. Since $k_{\text{T}}^2/[x(1-x)]$ gives the virtuality (Q^2) of the mother parton, the formation time can also be written as $\tau_{\text{form}} = 2E/Q^2$. Since the uncertainty principle $\Delta x \Delta p \sim 1$ has been used to obtain Eq. (1), one should treat this relation as an approximation of the same order. Therefore, it is necessary to understand the sensitivity of jet energy loss to the exact values one applies for the formation time. In literature, $\tau_{\text{form}} \sim 2E/k_{\perp}^2$ is also frequently used by assuming that k_{\perp}^2 and Q^2 are on the same order.

To study the effects of parton formation time on jet quenching, we compare our calculations between three different estimations of this formation time.

- **Setup 1: zero formation time** – the vacuum shower is assumed to happen instantaneously ($\tau_1 = 0$) and jet partons start interact with the QGP when the hydrodynamic evolution of the QGP commences (at τ_0).
- **Setup 2: formation time from single splitting** – each parton is assumed to be formed from

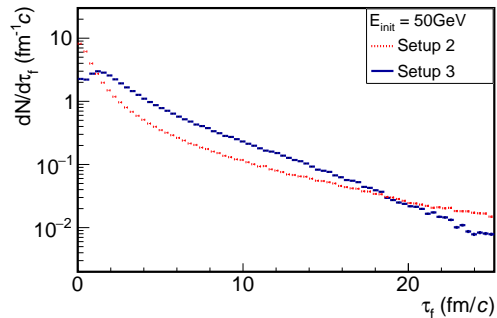


FIG. 1: (Color online) Distribution of final-state partons from Pythia emanating from a 50 GeV quark as functions of the formation time, compared between different setups.

one splitting which takes the time of $\tau_2 = 2Ex(1-x)/k_{\text{T}}^2$, where E represents the energy of the ancestor parton (directly produced by the initial hard scattering) at the top of the mother-daughter tree generated by Pythia shower, x and k_{T} are respectively the fractional energy and transverse momentum of the given final-state parton with respect to its ancestor; thus this jet parton starts to interact with the QGP at $t_{\text{init}} = \max(\tau_0, \tau_2)$.

- **Setup 3: formation time from multiple splittings** – the full sequence of splittings from the very first ancestor to each final-state parton in Pythia is tracked, and the parton formation time is calculated as $\tau_3 = \sum_i 2E_i x_i (1-x_i)/k_{\text{T}i}^2$, where E_i represents the energy of the mother parton in the i -th splitting, x_i and $k_{\text{T}i}$ are respectively the fractional energy and transverse momentum of a daughter with respect to the mother; thus this jet parton starts to interact with the QGP at $t_{\text{init}} = \max(\tau_0, \tau_3)$.

These setups are well defined for partons originating from the initial hard scattering process. For those from other sources in Pythia simulation, such as the initial state radiation, we set their formation time as zero in the present work.

In Fig. 1 we first study the formation time distribution of the final-state Pythia partons developed from a single quark at a fixed energy of 50 GeV and the maximum possible virtuality scale also of 50 GeV, compared between our setup-2 (single splitting) and setup-3 (sequential splittings). One would expect a δ -function at zero formation time for our setup-1 (instantaneous formation). Compared to setup-1, one observes that a large number of partons from setup-2 and 3 are formed during the QGP phase: there are only about 50% partons for setup-2 and 20% partons for setup-3 formed before ~ 1 fm/c (the scale of the initial time of the QGP); the amount increases to about 83% and 76% at the time around 5 fm/c and approaches about 90% and

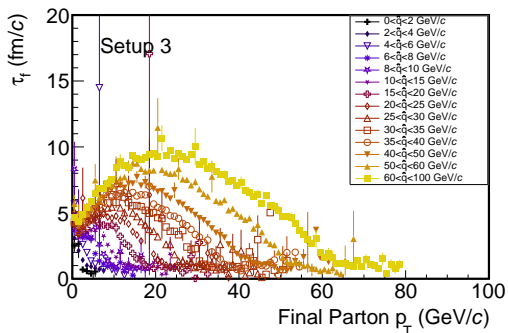


FIG. 2: (Color online) Dependence of the average formation time from sequential splittings (setup-3) on the final-state parton p_T , compared between different \hat{p}_T regions in Pythia for p+p collisions at $\sqrt{s} = 200$ GeV.

92% around 10 fm/c (the QGP lifetime). The remaining amount is formed out of the dense nuclear matter. Therefore, taking into account the parton formation time will significantly delay the jet-medium interaction and affect the jet quenching observables.

The difference in the formation time between our setup-2 and 3 originates from two competing effects. The addition of time for a sequence of splittings (setup-3) can lead to a longer formation time than that of a single splitting (setup-2). On the other hand, since both energy E and virtuality Q^2 (or k_{\perp}^2) in Eq. (1) drop after each splitting, it is possible that the formation time estimated from setup-2 is larger than that from setup-3. In general, the parton distributions are comparable (on the same order) over a wide range of formation time in Fig. 1. This can be understood with the dominating contribution to the total formation time from the last (softest) splitting. However, a closer comparison suggests, within the QGP lifetime ($1 \sim 10$ fm/c), partons from setup-3 tend to form later than those from setup-2.

To further investigate the dependence of formation time on the parton energy scale, in Fig. 2, we present the average formation time of partons as a function of their final state p_T generated by Pythia. Here, we simulate the proton-proton (p+p) collisions $\sqrt{s} = 200$ GeV and use our setup-3 for sequential splittings to calculate the parton formation time. Inside the figure, results from different \hat{p}_T bins are compared, which govern the amount of momentum exchange for the initial hard scatterings in Pythia and is around the initial p_T of partons directly produced from the hard splittings. From Fig. 2, we observe that for a given \hat{p}_T bin, the formation time first increases and then decreases as the final-state parton p_T increases. Since the hardest final-state partons are most likely produced via very few unbalanced splittings (or even no splitting) from the initial hard parton, they have very short formation time. On the other hand, medium p_T partons that approach mass shells after multiple splittings show longer formation time. We have also noticed

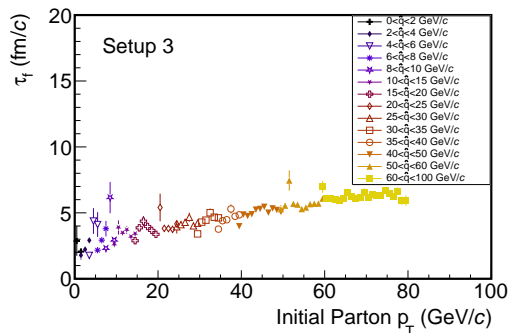


FIG. 3: (Color online) Dependence of the average formation time from sequential splittings (setup-3) on the initial-state parton p_T , compared between different \hat{p}_T regions in Pythia for p+p collisions at $\sqrt{s} = 200$ GeV.

that the longest formation time comes from splittings where daughter partons are almost collinear ($k_T \rightarrow 0$). The peak value of the formation time becomes larger as one increases the initial \hat{p}_T bin. This is because partons produced from more energetic collisions usually possess higher virtualities thus take longer time to shower towards their mass shells.

The same conclusions can also be drawn from Fig. 3 where we present the average formation time as a function of the p_T of the ancestor partons directly produced from hard collisions in Pythia. In the figure, one can clearly observe the mapping between the \hat{p}_T bins and the ranges of the ancestor parton p_T . With the increase of this initial p_T , the average time for shower partons to approach their mass shells becomes longer. An approximately linear relation is seen between the average formation time of the shower partons and the initial p_T of the ancestor partons. We have confirmed that the parton formation time estimated using our setup-2 (single splitting scenario) shares the similar dependences on the initial and final state parton p_T to setup-3 here.

III. NUCLEAR MODIFICATION OF JETS

The final-state partons generated by Pythia are fed into the linear Boltzmann transport (LBT) model [32, 74] for their subsequent interactions with the QGP medium. In LBT, the phase space distribution of jet partons (denoted by “ a ” here) is evolved according to the Boltzmann equation

$$p_a \cdot \partial f_a = E_a (\mathcal{C}_{el} + \mathcal{C}_{inel}), \quad (2)$$

where the collision term on the right hand side includes contributions from both elastic and inelastic processes. The elastic scatterings between jet partons and thermal partons inside the QGP are modeled according to the leading-order (LO) perturbative QCD (pQCD) matrix elements that take into account all possible $2 \rightarrow 2$

channels [78], while the inelastic scatterings are modeled based on the higher-twist energy loss calculation of medium-induced gluon emission [11, 17, 79]. The only parameter we adjust for LBT in this work is the strong coupling constant α_s , which directly affects the interaction strength in elastic scatterings, and controls the rate of medium-induced gluon through the jet transport coefficient \hat{q} that characterizes the transverse momentum broadening square per unit time due to elastic scatterings.

For realistic heavy-ion collisions, the spatial distribution of initial jets is calculated according to the binary collision vertices from the Monte-Carlo (MC) Glauber model. The QGP is simulated using a viscous hydrodynamic model (VISHNew [80–82] in this work) that is initialized with the MC Glauber model for its entropy density distribution. The initial time of the hydrodynamic evolution is set as $\tau_0 = 0.6$ fm/c, and the specific shear viscosity is set as $\eta/s = 0.08$ for a reasonable description of the soft hadron observables at RHIC and LHC. This hydrodynamic model provides the spacetime information of the local temperature and flow velocity of the QGP medium, based on which we obtain the momentum distribution of thermal partons that enters the collision term on the right hand side of Eq. (2).

In the LBT model, we not only track the phase space evolution of the jet partons and their emitted gluons, but also the thermal partons that are scattered out of the QGP background. The latter is denoted as “recoil” partons. In addition, generation of these recoil partons leaves particle holes inside the QGP, which are denoted as back-reaction or “negative” partons, and also tracked inside LBT in order to guarantee the energy-momentum conservation of the parton system. Recoil and negative partons constitute the “jet-induced medium excitation” and have been shown essential in understanding observables related to fully reconstructed jets [44, 45]. At the chemical freezeout hypersurface ($T_c = 165$ MeV), all partons discussed above are collected for jet reconstruction and observable analysis. Their further interactions with the hadron gas is neglected, considering its much more dilute density compared to the QGP medium.

For jet reconstruction, we feed all partons from Pythia (for p+p collisions) or Pythia+LBT (for heavy-ion, or A+A, collisions) into the Fastjet package with the anti- k_T algorithm selected [83, 84]. In this work, particles in the mid-rapidity $|\eta| < 1$ and $p_T > 0.2$ GeV/c are used for constructing jets. With a given jet cone size R , the reconstructed jet η_{jet} is required to be at R distance away from the acceptance edge as $|\eta_{\text{jet}}| < 1 - R$, so that the full jet locates inside the acceptance coverage. Note that the energy-momentum of the negative partons produced by LBT is subtracted from the reconstructed jets, similar to subtracting the medium background.

Shown in Fig. 4 is the nuclear modification factor R_{AA} of full jets with a cone size $R = 0.2$ in the top 10% Au-Au collisions at $\sqrt{s_{NN}} = 200$ GeV. Between different panels, we compare our three setups of the parton formation

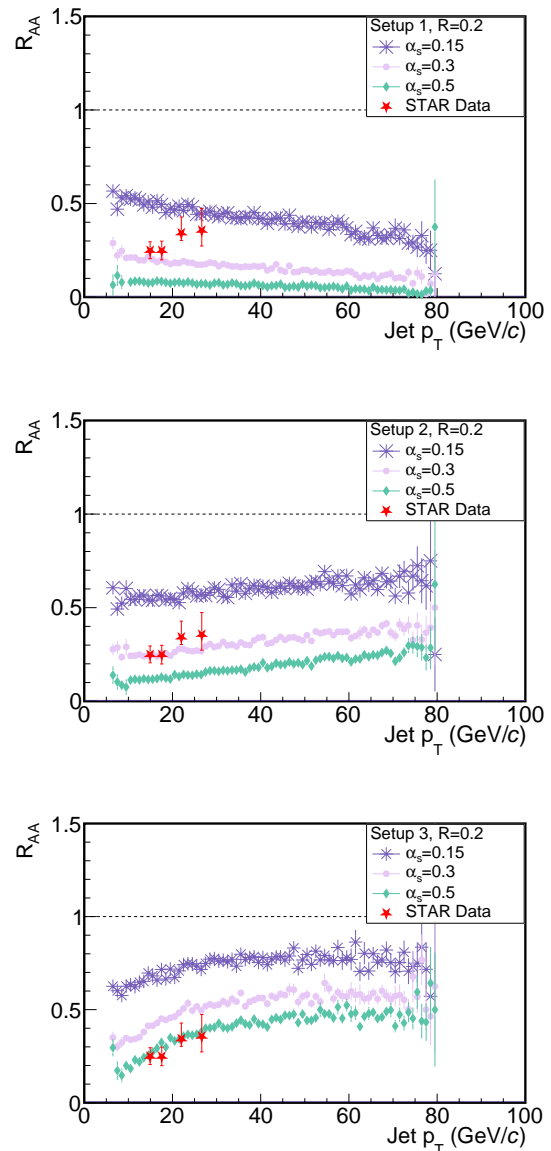


FIG. 4: (Color online) Nuclear modification factor R_{AA} of jets in 0-10% Au+Au collisions at $\sqrt{s_{NN}} = 200$ GeV, compared between using different α_s values and different setups of the parton formation time – upper panel for setup-1, middle for setup-2 and lower for setup-3.

time, upper panel for instantaneous formation (setup-1), middle for single splitting (setup-2) and lower for sequential splittings (setup-3). In each panel, results from using different α_s values are compared. For a given setup of formation time, the jet R_{AA} becomes smaller with an increasing value of α_s due to stronger jet-medium interactions. Meanwhile, with the same α_s value, we observe an increasing R_{AA} from top to bottom panels, because a longer formation time ($t_{\text{init}}^{\text{setup-3}} > t_{\text{init}}^{\text{setup-2}} > t_{\text{init}}^{\text{setup-1}}$) delays the medium modification on jets. Similar trend of larger R_{AA} with later jet formation time was also ob-

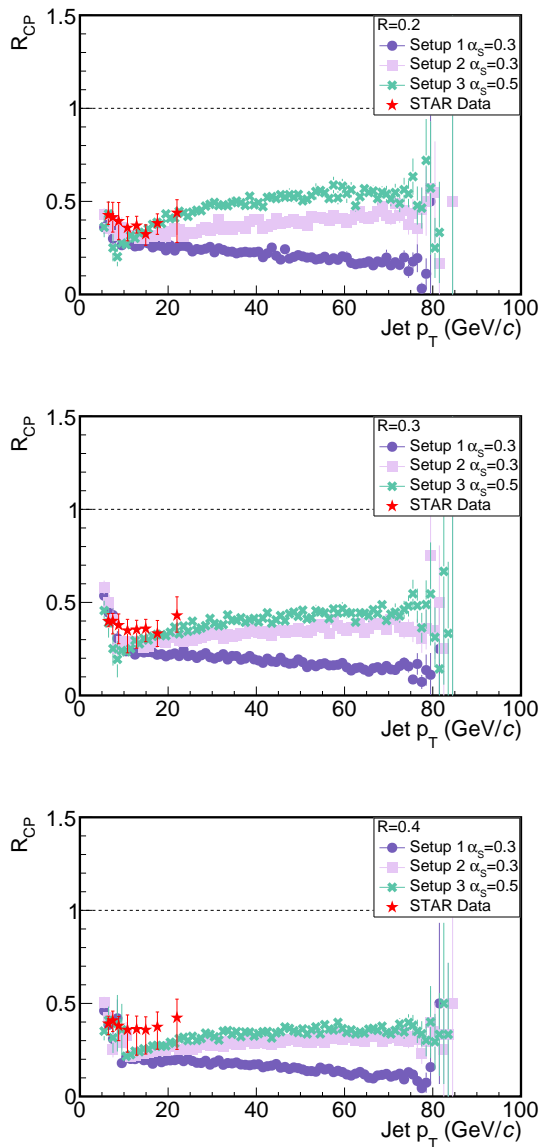


FIG. 5: (Color online) Central (0-10%) to peripheral (60-80%) ratio (R_{cp}) of jets in Au+Au collisions at $\sqrt{s_{NN}} = 200$ GeV, compared between different setups of the parton formation time at different jet cone sizes, upper panel for $R = 0.2$, middle for $R = 0.3$ and lower for $R = 0.4$.

served in Ref. [70]. In addition to the overall magnitude of jet quenching, here we also notice the p_T dependence of the jet R_{AA} can be affected by different assumptions of the parton formation time. At the RHIC energy, the jet R_{AA} would decrease with p_T if instantaneous formation is assumed (upper panel). However, by adopting a more realistic modeling of formation time, a slightly rising trend of R_{AA} with respect to p_T is seen. This can be understood with the larger formation time for higher p_T partons, as previously discussed in Figs. 2 and 3. This effect on the p_T dependence of the jet R_{AA} does not de-

pend on the α_s value we use here. Note that the STAR data [85] of R_{AA}^{Pythia} (ratio of jet spectra between measurement in A+A collisions and Pythia simulation) are also included in Fig. 4 as a reference. However, as discussed earlier, we are not attempting to precisely constrain the formation time from data in this work yet, considering that our current model calculation is still incomplete. For instance, jet partons at high virtuality (before arriving at their mass shells) can also lose energy inside the QGP [86, 87], which has not been taken into account in our current study. Therefore, results from our setup-3 in the lower panel of Fig. 4 do not conclude the coupling strength should be as strong as $\alpha_s = 0.5$. In addition, due to the challenge remaining in hadronizing jet partons in heavy-ion collisions, uncertainties exist in comparing our partonic jets in the present study to the charged jets with a high p_T hadron trigger measured by STAR. These will be improved in our future efforts.

To avoid uncertainties introduced by lacking the p+p baseline of jet measurement, one may also quantify the nuclear modification effect using the central-to-peripheral ratio (R_{cp}) of the jet spectra in A+A collisions. Shown in Fig. 5 is our calculation on this R_{cp} between 0-10% and 60-80% centrality bins, compared to the STAR data [85]. From the top to the bottom panel, we present results for different jet cone sizes – $R = 0.2$, 0.3 and 0.4 respectively. In each panel, we compare between our three setups of the formation time estimation. Similar to the jet R_{AA} previously presented in Fig. 4, we find that different modelings of the parton formation time affect not only the overall magnitude, but also the p_T dependence of the jet R_{cp} . Our setup-1, instantaneous parton formation, leads to a decreasing jet R_{cp} with respect to its p_T , which is disfavored by the STAR data. On the other hand, the increasing trend of R_{cp} with the jet p_T from more realistic evaluations of the formation time (setup-2 and 3) appear qualitatively consistent with the experimental observation.

IV. SUMMARY

In this paper, we have explored the impact of the parton shower formation time on jet quenching in relativistic heavy-ion collisions. The Pythia event generator is utilized to obtain parton showers in vacuum, based on which three different modelings have been set up to estimate the formation time of each parton, including instantaneous formation (setup-1), formation from single splitting (setup-2) and sequential splittings (setup-3). The final-state partons from Pythia are then fed into the LBT model for their subsequent interactions with the QGP medium.

Within this framework, we find that after considering the time taken by realistic splittings (for both setup-2 and 3), only a limited number of partons within jets form prior to the QGP formation, while a large number form inside and even after the QGP stage. The formation

time becomes longer as the scale of the momentum exchange in the initial hard scatterings increases. Within the lifetime of the QGP produced at the RHIC energy, we find the average parton formation time follows the hierarchy of $t_{\text{init}}^{\text{setup-3}} > t_{\text{init}}^{\text{setup-2}} > t_{\text{init}}^{\text{setup-1}}$, which leads to an inverse hierarchy of parton energy loss inside the QGP. Sizable effects can be seen on both the overall magnitude and the transverse momentum dependence of the nuclear modification factor of jets. For a given value of α_s , a smaller R_{AA} is seen with a shorter formation time. The jet R_{AA} decreases with p_T within our setup-1, while increases with p_T within our setup-2 and 3, due to a longer average parton formation time from a more energetic jet. Consistent results are observed across different α_s values, as well as for the central-to-peripheral ratio of the jet spectra (R_{cp}).

While our study has provided a detailed demonstration on the sensitivity of jet quenching observables to the formation time of parton showers, it requires further improvements in several directions in order to achieve

quantitative constraints on the parton formation time from the jet quenching data. For instance, instead of the free-streaming assumption, it is necessary to introduce medium modification on jet partons during their high virtuality stage to avoid possible underestimation of jet quenching, especially when the parton formation time is long. A solid hadronization scheme should also be introduced for a more direct comparison between our current model calculation at the parton level and the experimental measurements on the charged hadron jets.

Acknowledgments

We thank Yayun He, Tan Luo, Weiyao Ke, Maowu Nie and Xin-Nian Wang for helpful discussions. This work is supported by the National Natural Science Foundation of China (NSFC) under Grant Nos. 12175122, 2021-867, 11890710 and 11890713.

-
- [1] M. Gyulassy and L. McLerran, Nucl. Phys. A **750**, 30 (2005), arXiv:nucl-th/0405013.
 - [2] P. Jacobs and X.-N. Wang, Prog. Part. Nucl. Phys. **54**, 443 (2005), arXiv:hep-ph/0405125.
 - [3] W. Busza, K. Rajagopal, and W. van der Schee, Ann. Rev. Nucl. Part. Sci. **68**, 339 (2018), arXiv:1802.04801.
 - [4] G.-Y. Qin and X.-N. Wang, Int. J. Mod. Phys. **E24**, 1530014 (2015), arXiv:1511.00790.
 - [5] S. Cao and X.-N. Wang, Rept. Prog. Phys. **84**, 024301 (2021), arXiv:2002.04028.
 - [6] M. Connors, C. Nattrass, R. Reed, and S. Salur, Rev. Mod. Phys. **90**, 025005 (2018), arXiv:1705.01974.
 - [7] X.-N. Wang and M. Gyulassy, Phys. Rev. Lett. **68**, 1480 (1992).
 - [8] M. Gyulassy and X.-N. Wang, Nucl. Phys. **B420**, 583 (1994), nucl-th/9306003.
 - [9] B. G. Zakharov, JETP Lett. **65**, 615 (1997), hep-ph/9704255.
 - [10] R. Baier, Y. L. Dokshitzer, A. H. Mueller, and D. Schiff, Phys. Rev. **C58**, 1706 (1998), arXiv:hep-ph/9803473.
 - [11] X.-N. Wang and X.-F. Guo, Nucl. Phys. **A696**, 788 (2001), arXiv:hep-ph/0102230.
 - [12] P. Arnold, G. D. Moore, and L. G. Yaffe, JHEP **06**, 030 (2002), hep-ph/0204343.
 - [13] M. Gyulassy, I. Vitev, X.-N. Wang, and B.-W. Zhang, (2003), arXiv:nucl-th/0302077.
 - [14] A. Kovner and U. A. Wiedemann, (2003), arXiv:hep-ph/0304151.
 - [15] G.-Y. Qin *et al.*, Phys. Rev. Lett. **100**, 072301 (2008), arXiv:0710.0605.
 - [16] S. A. Bass *et al.*, Phys. Rev. **C79**, 024901 (2009), arXiv:0808.0908.
 - [17] A. Majumder, Phys. Rev. **D85**, 014023 (2012), arXiv:0912.2987.
 - [18] N. Armesto *et al.*, Phys. Rev. **C86**, 064904 (2012), arXiv:1106.1106.
 - [19] Y.-Y. Zhang, G.-Y. Qin, and X.-N. Wang, Phys. Rev. **D100**, 074031 (2019), arXiv:1905.12699.
 - [20] C. Sirimanna, S. Cao, and A. Majumder, Phys. Rev. C **105**, 024908 (2022), arXiv:2108.05329.
 - [21] R. Baier, Nucl. Phys. **A715**, 209 (2003), arXiv:hep-ph/0209038.
 - [22] A. Majumder, Phys. Rev. **C80**, 031902 (2009), arXiv:0810.4967.
 - [23] JET, K. M. Burke *et al.*, Phys. Rev. C **90**, 014909 (2014), arXiv:1312.5003.
 - [24] JETSCAPE, S. Cao *et al.*, Phys. Rev. C **104**, 024905 (2021), arXiv:2102.11337.
 - [25] M. Xie, W. Ke, H. Zhang, and X.-N. Wang, (2022), arXiv:2206.01340.
 - [26] I. Vitev and M. Gyulassy, Phys. Rev. Lett. **89**, 252301 (2002), arXiv:hep-ph/0209161.
 - [27] C. A. Salgado and U. A. Wiedemann, Phys. Rev. **D68**, 014008 (2003), hep-ph/0302184.
 - [28] A. Dainese, C. Loizides, and G. Paic, Eur. Phys. J. **C38**, 461 (2005), arXiv:hep-ph/0406201.
 - [29] S. Wicks, W. Horowitz, M. Djordjevic, and M. Gyulassy, Nucl. Phys. **A784**, 426 (2007), arXiv:nucl-th/0512076.
 - [30] N. Armesto, A. Dainese, C. A. Salgado, and U. A. Wiedemann, Phys. Rev. **D71**, 054027 (2005), arXiv:hep-ph/0501225.
 - [31] X.-F. Chen, T. Hirano, E. Wang, X.-N. Wang, and H. Zhang, Phys. Rev. **C84**, 034902 (2011), arXiv:1102.5614.
 - [32] S. Cao, T. Luo, G.-Y. Qin, and X.-N. Wang, Phys. Lett. **B777**, 255 (2018), arXiv:1703.00822.
 - [33] W.-J. Xing, S. Cao, G.-Y. Qin, and H. Xing, Phys. Lett. B **805**, 135424 (2020), arXiv:1906.00413.
 - [34] ATLAS, G. Aad *et al.*, Phys. Rev. Lett. **114**, 072302 (2015), arXiv:1411.2357.
 - [35] CMS, V. Khachatryan *et al.*, Phys. Rev. **C96**, 015202 (2017), arXiv:1609.05383.
 - [36] G.-Y. Qin and B. Muller, Phys. Rev. Lett. **106**, 162302 (2011), arXiv:1012.5280, [Erratum: Phys. Rev.

- Lett.108,189904(2012)].
- [37] C. Young, B. Schenke, S. Jeon, and C. Gale, Phys. Rev. C **84**, 024907 (2011), arXiv:1103.5769.
- [38] W. Dai, I. Vitev, and B.-W. Zhang, Phys. Rev. Lett. **110**, 142001 (2013), arXiv:1207.5177.
- [39] X.-N. Wang and Y. Zhu, Phys. Rev. Lett. **111**, 062301 (2013), arXiv:1302.5874.
- [40] J.-P. Blaizot, E. Iancu, and Y. Mehtar-Tani, Phys. Rev. Lett. **111**, 052001 (2013), arXiv:1301.6102.
- [41] Y. Mehtar-Tani and K. Tywoniuk, Phys. Lett. **B744**, 284 (2015), arXiv:1401.8293.
- [42] S. Cao and A. Majumder, Phys. Rev. C **101**, 024903 (2020), arXiv:1712.10055.
- [43] Z.-B. Kang, F. Ringer, and I. Vitev, Phys. Lett. **B769**, 242 (2017), arXiv:1701.05839.
- [44] Y. He *et al.*, Phys. Rev. **C99**, 054911 (2019), arXiv:1809.02525.
- [45] Y. He *et al.*, (2022), arXiv:2201.08408.
- [46] JETSCAPE, A. Kumar *et al.*, (2022), arXiv:2204.01163.
- [47] R. Perez-Ramos and T. Renk, Phys. Rev. **D90**, 014018 (2014), arXiv:1401.5283.
- [48] I. P. Lokhtin, A. A. Alkin, and A. M. Snigirev, Eur. Phys. J. **C75**, 452 (2015), arXiv:1410.0147.
- [49] Y.-T. Chien and I. Vitev, JHEP **05**, 023 (2016), arXiv:1509.07257.
- [50] J. Casalderrey-Solana, D. Gulhan, G. Milhano, D. Pablos, and K. Rajagopal, JHEP **03**, 135 (2017), arXiv:1609.05842.
- [51] Y. Tachibana, N.-B. Chang, and G.-Y. Qin, Phys. Rev. **C95**, 044909 (2017), arXiv:1701.07951.
- [52] R. Kunnawalkam Elayavalli and K. C. Zapp, JHEP **07**, 141 (2017), arXiv:1707.01539.
- [53] C. Park, S. Jeon, and C. Gale, Nucl. Phys. **A982**, 643 (2019), arXiv:1807.06550.
- [54] T. Luo, S. Cao, Y. He, and X.-N. Wang, Phys. Lett. **B782**, 707 (2018), arXiv:1803.06785.
- [55] N.-B. Chang, S. Cao, and G.-Y. Qin, Phys. Lett. **B781**, 423 (2018), arXiv:1707.03767.
- [56] Y. Mehtar-Tani and K. Tywoniuk, JHEP **04**, 125 (2017), arXiv:1610.08930.
- [57] G. Milhano, U. A. Wiedemann, and K. C. Zapp, Phys. Lett. **B779**, 409 (2018), arXiv:1707.04142.
- [58] P. Caucal, E. Iancu, and G. Soyez, JHEP **10**, 273 (2019), arXiv:1907.04866.
- [59] W. Chen, S. Cao, T. Luo, L.-G. Pang, and X.-N. Wang, Phys. Lett. B **810**, 135783 (2020), arXiv:2005.09678.
- [60] ATLAS, G. Aad *et al.*, Phys. Rev. Lett. **105**, 252303 (2010), arXiv:1011.6182.
- [61] CMS, S. Chatrchyan *et al.*, Phys. Lett. **B718**, 773 (2013), arXiv:1205.0206.
- [62] G.-Y. Qin, J. Ruppert, C. Gale, S. Jeon, and G. D. Moore, Phys. Rev. **C80**, 054909 (2009), arXiv:0906.3280.
- [63] L. Chen, G.-Y. Qin, S.-Y. Wei, B.-W. Xiao, and H.-Z. Zhang, Phys. Lett. **B773**, 672 (2017), arXiv:1607.01932.
- [64] L. Chen, G.-Y. Qin, S.-Y. Wei, B.-W. Xiao, and H.-Z. Zhang, Phys. Lett. **B782**, 773 (2018), arXiv:1612.04202.
- [65] W. Chen, S. Cao, T. Luo, L.-G. Pang, and X.-N. Wang, Phys. Lett. B **777**, 86 (2018), arXiv:1704.03648.
- [66] S.-L. Zhang, T. Luo, X.-N. Wang, and B.-W. Zhang, Phys. Rev. **C98**, 021901 (2018), arXiv:1804.11041.
- [67] Z.-B. Kang, J. Reiten, I. Vitev, and B. Yoon, Phys. Rev. D **99**, 034006 (2019), arXiv:1810.10007.
- [68] Z. Yang *et al.*, Phys. Rev. Lett. **127**, 082301 (2021), arXiv:2101.05422.
- [69] A. Luo, Y.-X. Mao, G.-Y. Qin, E.-K. Wang, and H.-Z. Zhang, (2021), arXiv:2109.14314.
- [70] L. Apolinário, A. Cordeiro, and K. Zapp, Eur. Phys. J. C **81**, 561 (2021), arXiv:2012.02199.
- [71] S. P. Adhya, C. A. Salgado, M. Spousta, and K. Tywoniuk, Eur. Phys. J. C **82**, 20 (2022), arXiv:2106.02592.
- [72] T. Sjöstrand *et al.*, Comput. Phys. Commun. **191**, 159 (2015), arXiv:1410.3012.
- [73] T. Sjostrand, S. Mrenna, and P. Z. Skands, JHEP **0605**, 026 (2006), arXiv:hep-ph/0603175.
- [74] S. Cao, T. Luo, G.-Y. Qin, and X.-N. Wang, Phys. Rev. C **94**, 014909 (2016), arXiv:1605.06447.
- [75] Z. Yang, T. Luo, W. Chen, L.-G. Pang, and X.-N. Wang, (2022), arXiv:2203.03683.
- [76] STAR, J. Adam *et al.*, Phys. Rev. D **101**, 052004 (2020), arXiv:1912.08187.
- [77] A. Adil and I. Vitev, Phys. Lett. B **649**, 139 (2007), arXiv:hep-ph/0611109.
- [78] J. Auvinen, K. J. Eskola, and T. Renk, Phys. Rev. **C82**, 024906 (2010), arXiv:0912.2265.
- [79] B.-W. Zhang, E. Wang, and X.-N. Wang, Phys. Rev. Lett. **93**, 072301 (2004), arXiv:nucl-th/0309040.
- [80] H. Song and U. W. Heinz, Phys. Lett. B **658**, 279 (2008), arXiv:0709.0742.
- [81] H. Song and U. W. Heinz, Phys. Rev. **C77**, 064901 (2008), arXiv:0712.3715.
- [82] Z. Qiu, C. Shen, and U. Heinz, Phys. Lett. **B707**, 151 (2012), arXiv:1110.3033.
- [83] M. Cacciari and G. P. Salam, Phys. Lett. B **641**, 57 (2006), arXiv:hep-ph/0512210.
- [84] M. Cacciari, G. P. Salam, and G. Soyez, Eur. Phys. J. **C72**, 1896 (2012), arXiv:1111.6097.
- [85] STAR, J. Adam *et al.*, Phys. Rev. C **102**, 054913 (2020), arXiv:2006.00582.
- [86] JETSCAPE, S. Cao *et al.*, Phys. Rev. C **96**, 024909 (2017), arXiv:1705.00050.
- [87] S. Cao, C. Sirimanna, and A. Majumder, (2021), arXiv:2101.03681.